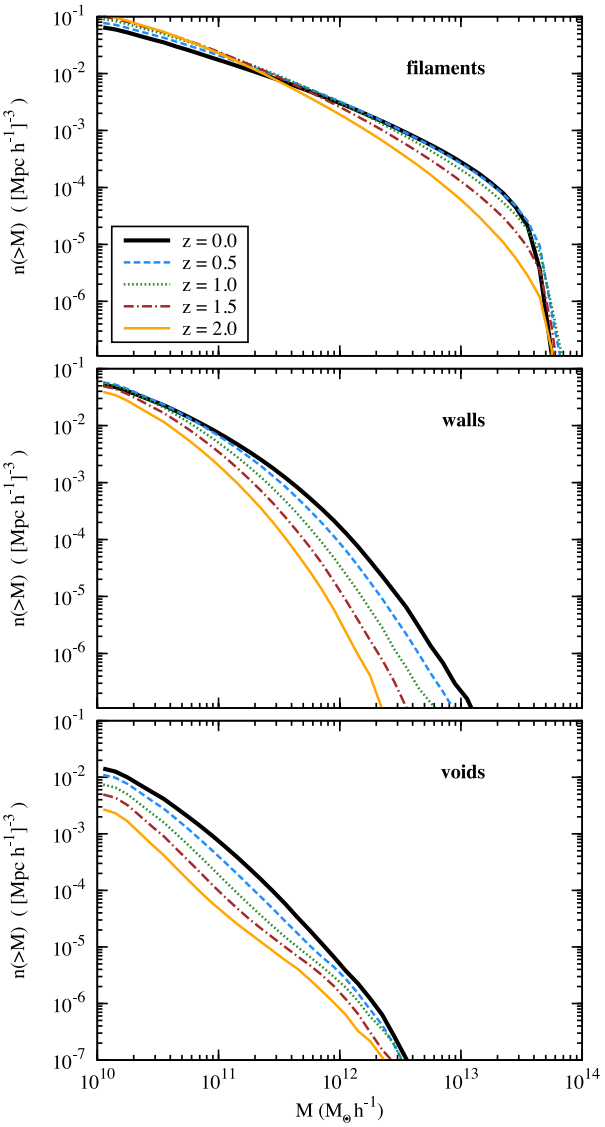

Figure 31. The evolution of the mass function for haloes residing in filament (top), wall (centre) and void (bottom) environments. The mass function is normalized to the entire volume of the simulation.

are more cluster regions, but that the cosmic web nodes contain many more massive haloes.

In contrast to node regions, the halo population across filaments shows a much slower evolution, as can be assessed from Fig. 31. The largest changes take place at high halo masses, with the population of such objects showing a considerable increase in number. The trend is reversed at lower masses suggesting that many small haloes are accreted by their more massive counterparts and therefore feeding the growth of these massive haloes. The slow evolution of the filaments halo population is even more interesting given that the volume of filament halves since $z = 2$ till present time (see Fig. 23). It implies that the same number of haloes has a much more compact distribution at later times.

Both wall and void regions show a major increase in their halo numbers since high redshift. In the case of walls, the increase is most pronounced at the high mass tail, while for voids the largest variation is found in the number of low mass haloes. The rapid change in these populations indicate that same mass haloes living in wall and void regions are more likely to be younger than their counterparts found in filaments and clusters (Aragón-Calvo 2007; Hahn et al. 2007a,b). It also suggest that galaxies living in wall and void regions evolve more slowly that their higher density analogues and therefore probably correspond to earlier stages of the galaxy formation process. On account of this, a comparison between void galaxies and their higher density counterparts can offer insights into the dominant galaxy evolution mechanisms acting at different times, without the need of high redshift observations (Kreckel et al. 2011, 2012).

7 MASS TRANSPORT ACROSS THE COSMIC WEB

Following the time evolution of the cosmic web raises an important question: what is the path that matter follows before arriving into its present environment? This question is related to how gravitational collapse takes place for an anisotropic distribution of matter. According to gravitational instability theory (Zel'dovich 1970; Icke 1973; White & Silk 1979; Sheth et al. 2001; Shen et al. 2006), an overdense region first collapses along the direction with the largest positive eigenvalue of the deformation tensor to give rise to a pancake-like matter distribution. If the second largest eigenvalue is positive too, than a collapse along this second axis takes place resulting in filament-like regions. And last, regions with a third positive eigenvalues contract along the third direction to give rise to fully collapse objects. This sequence of events predicts a well-defined evolution of the matter distribution, with mass flowing from voids into walls, than into filaments and only in the last step into cosmic web nodes. The predictions of this standard view should be easily testable, given the identification of the cosmic web components at different redshifts.

We find that the majority of mass elements flow according to the predictions of the gravitational instability theory, from less dense to more dense environments. For example, most of the DM particles located in filaments at $z = 2$ are found at the present time in cluster and filament regions. Similarly, most wall particles either remain in their current environment or are accreted to filaments and clusters. This is easily seen with the help of Fig. 32, which shows the DM particles in a thin slice segregated according to their environment at $z = 2$ and 0. To illustrate the changing cosmic web environment, the particles at $z = 2$ are coloured according to their environment at present time, while the $z = 0$ particles are painted according to their environment at $z = 2$.

While the transport of most mass elements between cosmic web components is in accordance with the predictions of the anisotropic collapse theory, there are a few that show an opposite flow, from more dense to least dense morphological components. For example, several of the $z = 2$ filament particles in the top-left panel of Fig. 32 are classified as wall particles at $z = 0$. Similarly, a small fraction of $z = 2$ wall particles are found to reside in void regions at the present time. The common link between these outliers is that they populate tenuous filaments and walls. Therefore, rather than presenting a challenge to the standard theory of cosmic web evolution, such results reveal the difficulty in identifying filaments and walls in underdense regions. This challenge is clearly visible when comparing the results of the five identification methods shown in Fig. 1, since most differences arise in the detection of tenuous structures in void-like regions. Therefore, we suspect that the puzzling results

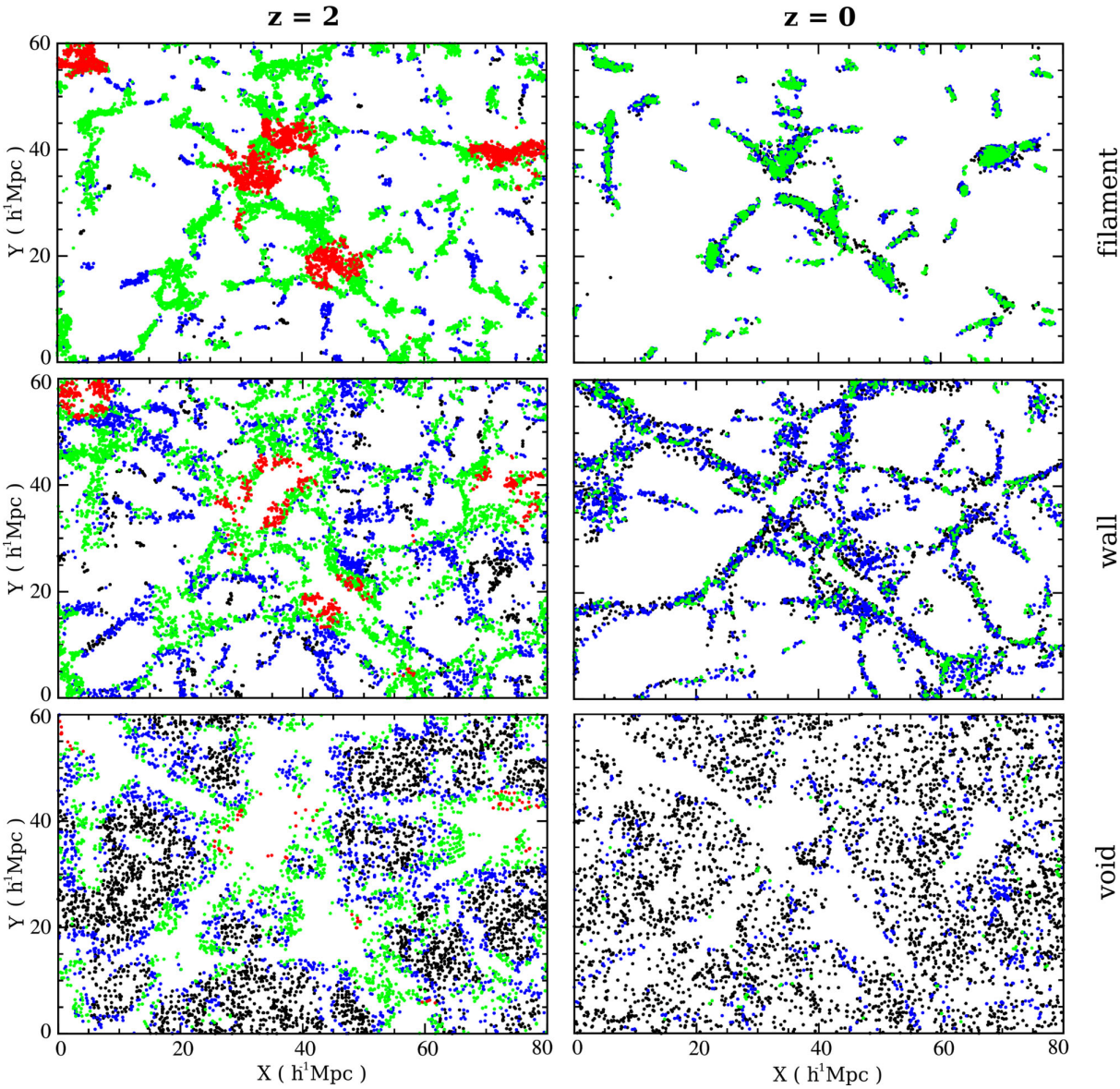

Figure 32. The DM particles segregated according to their environment at two different redshifts: $z = 2$ (left-hand column) and $z = 0$ (right-hand column). Each row shows only the particles located in: filaments (top row), walls (centre row) and voids (bottom row). The particles plotted at $z = 2$ (left-hand column) are coloured according to their environment tag at $z = 0$: cluster (red), filament (green), wall (blue) and void (black). Similarly, the particles shown at $z = 0$ are coloured according to their environment at $z = 2$, using the same colour scheme. The graph shows a small fraction, selected randomly, of the DM particles found in a $2\,h^{-1}$ Mpc thick slice.

are due to an incomplete or incorrect identification of environments in underdense regions.

Fig. 32 offered an intriguing, but only qualitative view on mass transport across morphological components. To undergo a more quantitative analysis, we define the common mass fraction between two cosmic web components at different times, i.e. between component i at redshift z_1 and component j at redshift z_2, as

$$f_{ij}(z_1, z_2) = \frac{M_{(i;z_1)\cap(j;z_2)}}{M_{i;z_1}}. \quad (16)$$

With $M_{i;z_1}$ we denoted the mass in environment i at redshift z_1, while $M_{(i;z_1)\cap(j;z_2)}$ denotes the mass overlap between cosmic web components i and j, with the first at redshift z_1 and the second at z_2. To compute the mass overlap we use the id tag of the DM particles to find all the common mass tracers between the two environments at different time steps of the simulation. The quantity $f_{ij}(z_1, z_2)$ has two common interpretations depending on the relation between z_1 and z_2.

(i) If $z_1 < z_2$, then the overlap fraction $f_{ij}(z_1, z_2)$ reveals what percentage of the z_1 mass in environment i originated from mass found in environment j at the higher redshift z_2.

(ii) If $z_1 > z_2$, then $f_{ij}(z_1, z_2)$ represents the fraction of z_1 mass in environment i that is found at a later time z_2 to be contained in environment j.

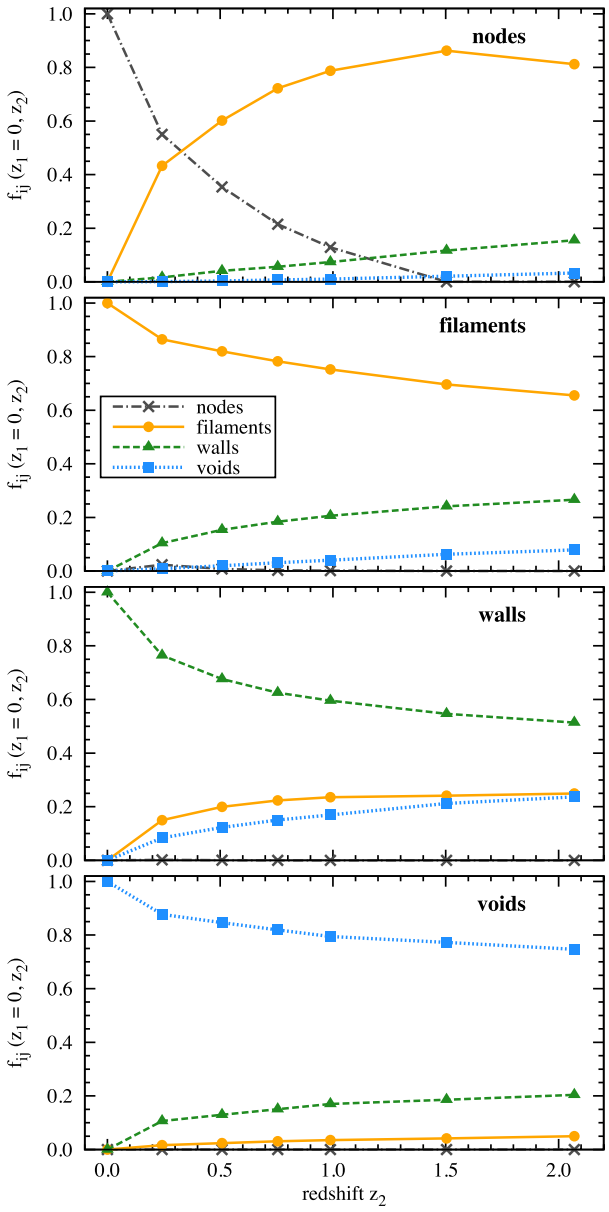

Figure 33. Tracing back in time which environments contributed to the current mass in cosmic web nodes (top row), filaments (second row), walls (third row) and voids (bottom row). The y-axis gives how the mass of a given environment at $z_1 = 0$ was split among the cosmic web components at a higher redshift z_2.

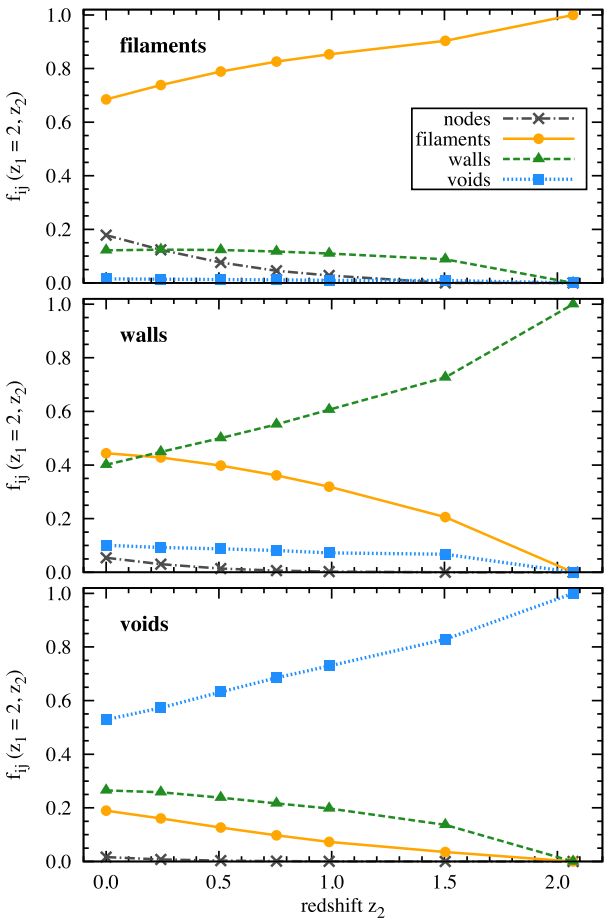

Figure 34. Tracking the final destination of the $z = 2$ mass found in cosmic web filaments (top), walls (centre) and voids (bottom). The y-axis gives how the mass in a given environment at $z_1 = 2$ was split among the cosmic web components at lower redshift z_2. Note that at $z = 2$ we do not find any cosmic nodes.

In Fig. 33 we investigate the morphological origin of the mass found in the present-day cosmic web environments. In the case of cosmic web nodes, most of their mass originated in filaments and only a small fraction of it in walls. This agrees very well with the standard picture according to which clusters accumulate mass from the filaments that have the cluster as one of their end points (e.g. Shandarin & Klypin 1984; Shandarin & Zeldovich 1989; van Haarlem & van de Weygaert 1993; Aubert & Pichon 2007; van de Weygaert & Bond 2008). Most of the mass in filaments seems to have been part of filamentary environments since early redshift, with only a small fraction coming from walls and voids. It has important implications for the population of filament haloes and galaxies since it implies that the majority of such objects have been in filament environments since at least $z = 2$.

Fig. 33 also characterizes the fraction of mass that changed environment in opposite way than predicted by the gravitational instability theory. As we already argued, this is indicative of the limitations of our method in the identification of tenuous structures. Quantifying this artefact is important in understanding if this drawback represents a serious problem for our analysis. We find that up to 20 per cent of present-day mass content of sheets has been identified as part of filaments at an earlier time, with a similar mislabelling of void mass content too. Therefore, the artefacts arising from the difficulty of detecting tenuous environments, though not dominant, cannot be neglected.

Fig. 34 shows another way of looking at the evolution of matter in the cosmic web. It plots the successive destinations of the matter that is initially, at $z = 2$, identified as being part of filaments, walls and voids. Compared to the previous figure, it illustrates the rapid outflow of mass from walls and voids. Less than 40 per cent of the walls $z = 2$ mass is still part of present-day's sheets, with most of the mass flowing into filaments. For voids, around half of their high redshift mass has streamed out into sheets and filaments, showing the significant outflow of mass from underdense regions.

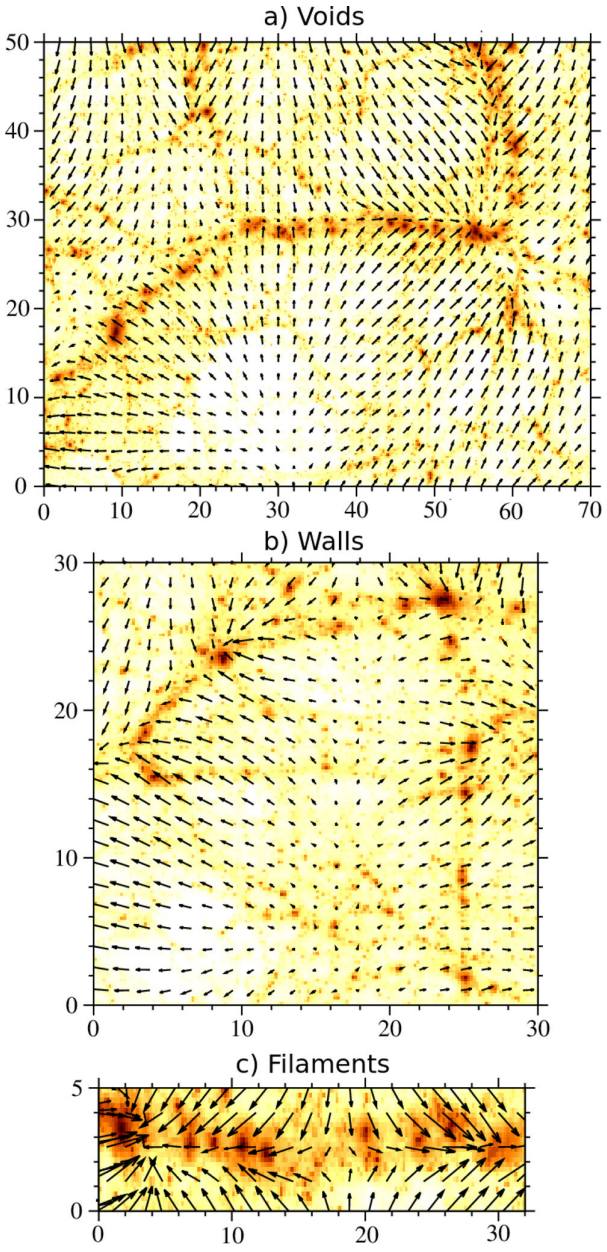

Figure 35. The velocity field along a few typical void (top), wall (centre) and filament (bottom right) stretches. The background image shows the density field, with light and dark patches corresponding to underdense and overdense regions. The arrows show the direction of the matter flow in the plane of the image, with the size of the arrow proportional to the velocity magnitude. Note that each panel has a different physical size as indicated by the coordinate ticks.

These results show that even though individual structures extended on tens of megaparsecs scales, the cosmic web components are evolving rapidly and are far from being static structures.

Fully understanding the mass transport across morphological components can only be done by investigating the large-scale velocity field, since this is the main driver behind megaparsec-scale mass flows. To that end, we present in Fig. 35 the peculiar velocity field across a few representative void, wall and filament stretches. The void regions are characterized by a strong outflow, with the velocity clearly pointing out towards the sheets that act as void boundaries. One such sheet is visible in the centre of panel (a), and it shows that the walls accrete mass from both of the two voids separated by the sheet. Moreover, the direction of the inflow is close to the normal to the wall, which resides along the horizontal line in the plane of the figure. This is true for most parts of the sheet, except close to large agglomerations of mass. Once in sheets, the matter outflows towards the filaments that border the wall, as clearly seen in panel (b) of Fig. 35. In filaments, the flow points towards the two massive clusters which act as the filament's endpoints.

According to the above velocity field, matter outflows from voids into walls, while the mass content of sheets streams towards filaments. In turn, the filaments act as matter transport highways towards the clusters bounding them. This is in very good agreement with both the predictions of anisotropic collapse theory and the mass transport results we obtained in this section. Moreover, it offers conclusive proof that the artificial transport of mass from filaments into walls or from walls into voids is an artefact of the cosmic web identification methods and does not pose a challenge to current cosmic web evolution theories.

8 SIZE AND DISTRIBUTION OF FILAMENTARY AND WALL NETWORKS

In the previous sections we characterized the evolution of the cosmic web in terms of both its mass and halo content, finding a marked time variation in these quantities. But these are not the only way of describing morphological components, since such structures also have certain spatial extents, which, according to Figs 21 and 22, show a significant evolution too. For this reason, this section is focused on characterizing the evolution in spatial extent of the filamentary and wall networks. We investigate the total length of the filament network as well as the typical diameter of these objects. Of particular interest is the density profile perpendicular to the filament spine and how this correlates to the filament width. The wall network undergoes a similar analysis, with studies of the total area of sheets and their typical thickness. At the end of this section we examine the spatial distribution of filaments and walls by performing a fractal dimensional analysis of these structures.

8.1 Total extent of filaments and walls

The most basic way of characterizing the spatial extent of morphological components is in terms of the length of filaments and area of sheets (e.g. Sousbie et al. 2008a; Pogosyan et al. 2009; Gay, Pichon & Pogosyan 2012). To that end, Fig. 36 shows the time variation of these quantities, which were computed using the procedures described in Sections 4.2.1 and 4.3.1. As expected, the overall length of filaments has decreased dramatically since high redshift. Nowadays, the filamentary network has only one-third of its extension compared to $z = 2$. Similarly, the total area of sheets has also decreased since high redshift, but only to a lesser extent. These findings are in very good agreement with the visual impression given by Figs 21 and 22, and reinforce the view that at later time both the filament and wall networks have a smaller extension.

More interestingly, the change in size of both filaments and walls seems to be almost independent of redshift. This is a puzzling result, given that qualitatively we find only a minor evolution of the cosmic web after $z = 0.5$ (see Figs 21 and 22). The answer to this may lie in the main limitation of the investigated quantities, since the total